

See discussions, stats, and author profiles for this publication at: <https://www.researchgate.net/publication/277352533>

The Liquid-Liquid Phase Transition and Its Phase Diagram in Deeply-Cooled Heavy Water Confined in a Nanoporous Silica Matrix

ARTICLE in JOURNAL OF PHYSICAL CHEMISTRY LETTERS · MAY 2015

Impact Factor: 7.46 · DOI: 10.1021/acs.jpcllett.5b00827

CITATIONS

2

READS

75

6 AUTHORS, INCLUDING:



Juscelino B. Leao

National Institute of Standards and Technol...

59 PUBLICATIONS 819 CITATIONS

SEE PROFILE



Leland W. Harriger

National Institute of Standards and Technol...

36 PUBLICATIONS 458 CITATIONS

SEE PROFILE



Yun Liu

National Institute of Standards and Technol...

115 PUBLICATIONS 3,877 CITATIONS

SEE PROFILE



Sow-Hsin Chen

Massachusetts Institute of Technology

469 PUBLICATIONS 15,629 CITATIONS

SEE PROFILE

Liquid–Liquid Phase Transition and Its Phase Diagram in Deeply-Cooled Heavy Water Confined in a Nanoporous Silica Matrix

Zhe Wang,[†] Kanae Ito,[†] Juscelino B. Leão,[‡] Leland Harriger,[‡] Yun Liu,^{‡,§} and Sow-Hsin Chen^{*,†}

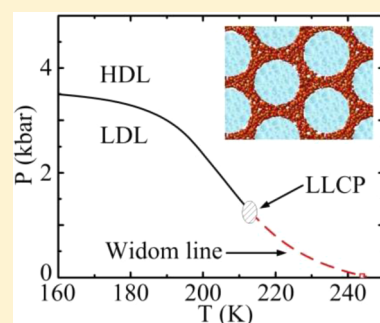
[†]Department of Nuclear Science and Engineering, Massachusetts Institute of Technology, Cambridge, Massachusetts 02139, United States

[‡]NIST Center for Neutron Research, National Institute of Standards and Technology, Gaithersburg, Maryland 20899, United States

[§]Department of Chemical Engineering, University of Delaware, Newark, Delaware 19716, United States

Supporting Information

ABSTRACT: Using neutron diffraction technique, we measure the average density of the heavy water confined in a nanoporous silica matrix, MCM-41, over the pressure–temperature plane. The result suggests the existence of a line of liquid–liquid phase transition with its end point at 1.29 ± 0.34 kbar and 213 ± 3 K in a fully hydrated sample. This point would be the liquid–liquid critical point (LLCP) according to the “liquid–liquid critical point” scenario. The phase diagram of the deeply cooled confined heavy water is then discussed. Moreover, in a partially hydrated sample, the phase transition completely disappears. This result shows that it is the free water part, rather than the bound water part, of the confined water that undergoes a liquid–liquid transition.



Water exhibits anomalous thermodynamic behaviors at low temperatures.^{1–4} When cooling, its thermodynamic response functions, such as isothermal compressibility, isobaric heat capacity, and isobaric thermal expansion coefficient, deviate from those of simple liquids significantly. These anomalies could be understood if one accepts that a first order low-density liquid (LDL) to high-density liquid (HDL) phase transition and the associated liquid–liquid critical point (LLCP) exist in the deeply cooled region of water.⁵ Unfortunately, the experimental detections of this liquid–liquid phase transition (LLPT) and its LLCP in bulk liquid water are almost impossible. It is because both the LLPT and LLCP are expected to exist below the homogeneous nucleation temperature T_H (235 K at 1 atm), where bulk water cannot be maintained in the liquid state. In order to enter this deeply cooled region of water, a hydrophilic nanoporous silica material, MCM-41, with 15-Å pore diameter is used to confine the water. Such “strong confinement” can suppress the homogeneous nucleation process and thus can keep the confined water in liquid state at least down to 130 K.⁶ Note that, the restricted geometry and the water–surface interactions are influential to the properties of the confined water. Therefore, to what extent the confined water is similar to the bulk water is still in debate.^{7–9} However, such a confined water system is of fundamental importance in practice and fascinates scientists from different disciplines. For example, it represents many biological and geological systems where water resides in nanoscopic pores or in the vicinity of hydrophilic or hydrophobic surfaces.

It is common that the first order phase transition exhibits metastability. Therefore, one can test the existence of the

hypothetical first order LLPT by detecting the hysteresis of the order parameter, the density of water. Recently, Zhang et al. attempted to detect the hypothetical LLPT in the heavy water confined in MCM-41.¹⁰ They measured the average density of the confined D₂O with warming and cooling scans at pressures from 1 bar to 2.9 kbar. The main result is shown in Figure 1 (the data at 3.3 k and 4 kbar in Figure 1 were measured with a similar method¹¹) and can be summarized as follows. (1) Density hysteresis phenomenon is observed at all the measured pressures below ~ 3.5 kbar. (2) When the pressure is below ~ 1.5 kbar, the hysteresis enhances as the pressure increases. The maximum density differences between the cooling and warming scans are 0.01 g/cm³ at 1 bar, 0.017 g/cm³ at 1 kbar, and 0.031 g/cm³ at 1.5 kbar, respectively. (3) When the pressure is above ~ 1.5 kbar, the amplitude of the hysteresis stabilizes at about 0.03 g/cm³. (4) The temperature of the maximum density difference between the cooling and warming scans shifts to lower temperature as the pressure increases. Zhang et al. attribute this strong hysteresis phenomena observed at pressures higher than ~ 1500 bar to the crossing of the LLPT line, due to the discontinuity at the phase boundary and the strong metastability of the liquid water in the coexisting region¹² as the result of the LLPT^{13,14} and to the confinement.^{15,16} The hysteresis observed below ~ 1000 bar, which are relatively weak, are attributed to possible temperature lags between the warming and cooling scans rather than to the crossing of a phase boundary. However, this conclusion was

Received: April 21, 2015

Accepted: May 13, 2015



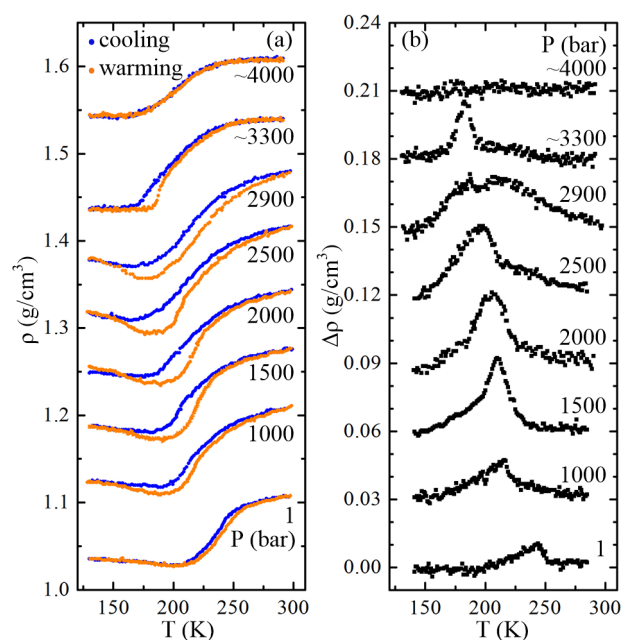


Figure 1. Density measurement on the confined D₂O made by Zhang et al.¹⁰ (1 bar to 2.9 kbar) and Wang et al.¹¹ (3.3 kbar and 4 kbar). (a) Density profiles of confined D₂O with warming and cooling scans at different pressures. The data are shifted by 0.05 g/cm³ between adjacent pressures for clarity. (b) Density differences between the cooling and warming scans at different pressures. The data are shifted by 0.03 g/cm³ between adjacent pressures for clarity.

soon challenged by Limmer and Chandler.¹⁷ With a computer simulation study employing mW model of water, these

researchers attribute all of the observed density hysteresis phenomena to a liquid–solid transition (LST) in the confined water (this result is also in debate^{18,19}). An important difference between the LLC scenario and LST scenario is that in the LLC scenario there is a LLC that terminates the LLPT line at a positive pressure. In contrast, in the LST scenario there is no associated critical point and the LST line exists in all the positive pressures.

In order to clarify the nature of the transition in the deeply cooled confined D₂O, we performed a series of neutron diffraction experiments to measure the average density of the D₂O confined in MCM-41 with warming and cooling scans at different pressures. The experiments were performed at the cold neutron spin polarized inelastic neutron spectrometer (SPINS) and a small-angle neutron scattering instrument (SANS) at National Institute of Standards and Technology Center for Neutron Research (NCNR). The full hydration level of the sample is $h = 0.5$ g/g (hydration level h is defined as (weight of water)/(weight of dry sample)). The method to extract the average density of the confined water from the neutron diffraction spectra is same to the one used in several previous studies.^{10,11,20–22} Detailed descriptions of the experimental method can be found in the Supporting Information.²³ In the study of Zhang et al.,¹⁰ the researchers performed the temperature scans with the following procedure: for each pressure, the sample was cooled from 300 to 130 K at ambient pressure and then pressurized to the desired value. After 2 h of waiting, the warming scan with 0.2 K/min was first performed from 130 to 300 K. When the warming scan was finished, they waited for another 2 h and then performed the cooling scan with 0.2 K/min from 300 to 130 K (the data at 3.3 and 4 kbar in Figure 1 are measured by similar protocol but

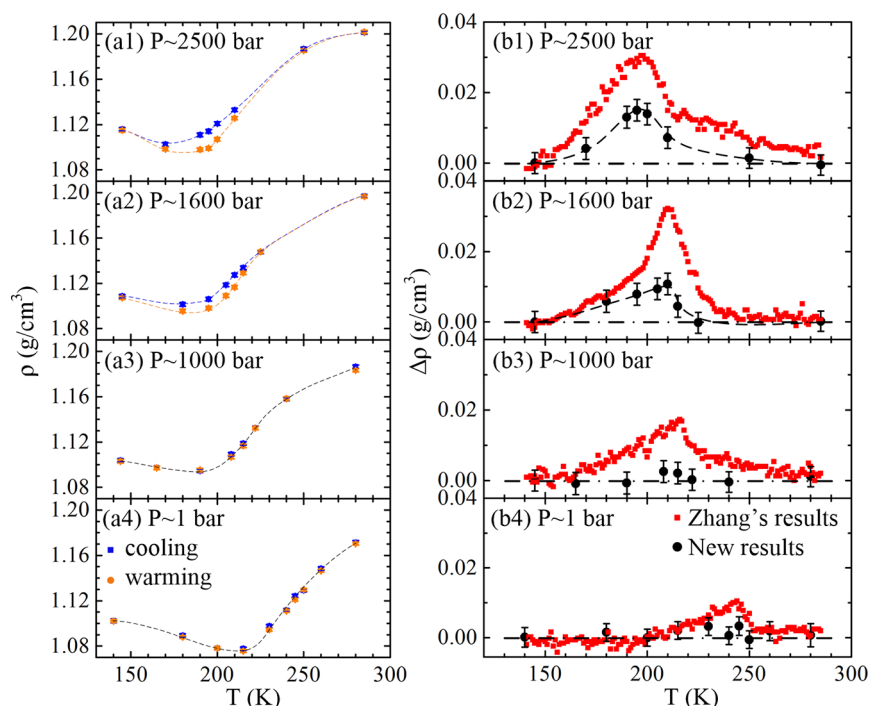


Figure 2. Density measurement on the confined D₂O with the new temperature scan protocol. The left column shows the density profiles with warming and cooling scans at $P \sim 2500$ bar (a1), 1600 bar (a2), 1000 bar (a3), and 1 bar (a4). The right column shows the density differences between the cooling and warming scans (denoted by black circles) at $P \sim 2500$ bar (b1), 1600 bar (b2), 1000 bar (b3), and 1 bar (b4). We also plot the results of the density differences in ref 10 (denoted by red circles) for comparison. The dashed lines are drawn to guide eyes. The data at 1 bar were taken at SANS, and the data at other pressures were taken at SPINS.

with cooling scan first¹¹). Note that, in such continuous temperature scans, the temperature changes continuously with constant speed. Though the speed is slow, it is possible that the heat transfer does not complete and the temperature sensor, which is on the aluminum holder of the sample, cannot accurately reflect the temperature of the confined water. In this case, there may be a temperature lag between the warming and cooling scans, and a hysteresis that is not due to the phase transition may appear. To eliminate the possible temperature lag, in this study, we use a new protocol for the temperature scan. For each pressure, we only measure several important temperatures around which the density hysteresis takes place. In addition, before each measurement, we wait for half an hour after the temperature reaches the desired value. Therefore, there is sufficient time for the sample to get a uniform temperature distribution and to reach temperature equivalence to the sample holder. The result of the density measurement with this new protocol is shown in Figure 2. It is found that the effective density hysteresis only appears when the pressure is higher than about 1500 bar. It takes place at the temperature that is very close to the one found in ref 10. This result suggests a first order transition between a low-density phase and a high-density phase and is consistent with the LLPT picture, rather than the LST picture. The end point of the phase separation, which locates at 1.29 ± 0.34 kbar and 213 ± 3 K, is the LLCP of the confined D_2O according to the LLCP scenario. In previous studies,^{24,25} we estimated the critical pressure of the confined H_2O to be 1.5 ± 0.3 kbar by the dynamical properties of the system. The critical pressure obtained here agrees with the previous estimations on the confined H_2O fairly well. Furthermore, above the critical pressure, the maximum density difference increases as the pressure increases (0.010 ± 0.003 g/cm³ at ~ 1.6 kbar; 0.016 ± 0.003 g/cm³ at ~ 2.5 kbar), which agrees with an idea that the phase separation becomes more significant as the distance from the critical point increases along the LLPT line.

We also tried other waiting times from 25 to 50 min for the density measurements at ~ 1.6 kbar. The result shows that the value of the average density of the confined D_2O is effectively constant for different waiting times used here. This observation suggests that after waiting for 25 min, the sample temperature becomes stable and no evident transition happens up to 50 min.

Below about 1000 bar, no effective hysteresis is observed in this study, which is different than the result in ref 10. This difference could be due to the temperature lag between the warming and cooling scans in the previous study. In principle, the influence of the temperature lag on the density measurement has a positive correlation with the isobaric heat capacity of the confined water (C_p). Therefore, the hysteresis at low pressures may indicate the maximum of C_p . This conjecture can be justified as follows. According to relevant thermodynamic studies,^{26,27} at ambient pressure, the peak position of C_p of the D_2O confined in MCM-41 with the pore diameter of 17 Å is 240 K. This value is very close to the temperature of the maximum density difference at ambient pressure in ref 10, which is 243 K (see Figure 2 (b4)). The small difference between these two temperatures may be due to the difference of the pore diameter. Notice that the peak position of C_p of the H_2O confined in MCM-41 is at 241 K with the pore diameter of 15 Å, and at 237 K with the pore diameter of 17 Å. Therefore, it seems that a 2-Å difference in pore diameter can change the temperature of the peak of C_p by several Kelvins.

Keep this idea in mind, one can then estimate the Widom line of the LLPT, which is defined as the locus of the C_p maxima in the corresponding one-phase region,²⁸ with the position of the maximum hysteresis observed at pressures lower than the critical pressure in ref 10. Note that, in many other literatures, the Widom line is defined as the locus of the maximum correlation length.^{29,30} This definition can avoid the confusion introduced by the existences of multiple local maxima in the heat capacity of water.³¹ However, in this study, we still employ the former definition because the heat capacity of the confined water is available, and thus, it is easy to compare our result to the result of thermodynamic measurement. In addition, as approaching the critical point, the maximum of heat capacity and the maximum of correlation length emerge.^{29,30}

Considering all the above discussions, we plot the phase diagram of the LLPT of the confined heavy water in Figure 3.

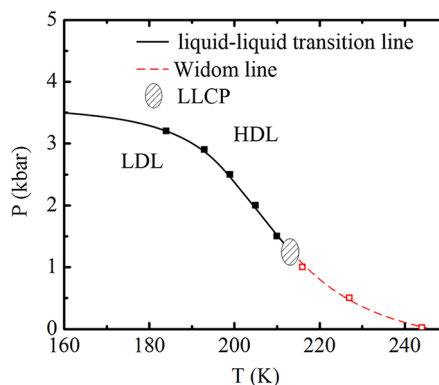


Figure 3. Phase diagram of the LLPT of the confined heavy water. The black solid squares and the red open squares denote the positions of the maximum density differences obtained by the continuous temperature scans at pressures higher than the critical pressure and lower than the critical pressure, respectively.^{10,11} The formers are due to the phase transition in the confined water and represent the LLPT line (denoted by a black solid line), whereas the latter ones are due to temperature lags and represent the Widom line (denoted by a red dashed line). These two lines intersect at the LLCP, whose approximate position is denoted by an elliptical region.

The black solid squares denote the positions of the maximum density differences obtained by the continuous temperature scans at pressures higher than the critical pressure.^{10,11} These hysteresis phenomena cannot be completely eliminated by the new temperature scan protocol introduced here and denote the LLPT of the confined water. By connecting these black solid squares with a smooth curve, and noting that the hysteresis disappears at pressures higher than 3500 bar in the temperature range from 140 to 300 K,¹¹ we obtain the LLPT line. The red open squares denote the positions of the maximum density differences obtained by the continuous temperature scans at pressures lower than the critical pressure.¹⁰ These hysteresis phenomena can be eliminated by the new protocol and denote the positions of the C_p maximum, that is, the Widom line. The LLPT line and the Widom line intersect at 1.29 ± 0.34 kbar and 213 ± 3 K. This point could be the LLCP according to the LLCP scenario.

It is believed that water undergoes glass transition at low temperatures.^{32,33} The transition temperature T_g is conjectured to be between 136^{34–36} and 165 K³⁷ for bulk water and 165 K for the water confined in MCM-41 at ambient pressure.²⁶ All of these temperatures are much lower than the temperatures at

which the hysteresis phenomena take place. Thus, the hysteresis should not be directly induced by the possible glass transition in the confined water. Another concern is that due to the possible existence of the glass transition, below the conjectured T_g the confined water may be in a glassy state, rather than an (metastable) equilibrium state, and the density measurement may be affected. In order to clarify this point, we perform a warming scan on density at 2 kbar by the following steps: first cool the system to 170 K at ambient pressure, then pressurize the system to 2 kbar and start the warming scan. In this route, the system temperature keeps on higher than the conjectured T_g of the confined water and the system should be always away from a glassy state. This experimental route gives an effectively same density profile as compared to the one obtained by the warming scan starting from 130 K. Therefore, we conclude that the hysteresis observed in this study is not affected by the possible glass transition in the confined water.

In order to examine the obtained phase diagram and to get a general idea on how the density of the confined water behaves as a function of T and P , we perform isobaric density measurements on the confined D_2O at five pressures: 0.1, 1, 2.5, 4, and 5 kbar. The data at 2.5 kbar are measured with warming scan. The results are shown in Figure 4. According to

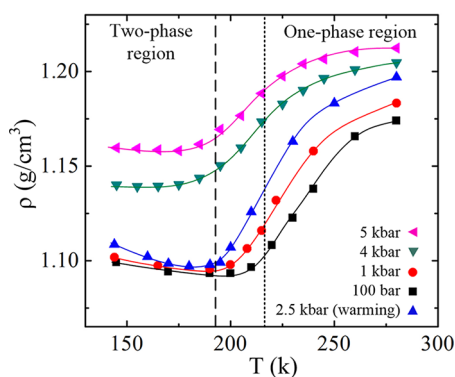


Figure 4. Average density of the confined D_2O as a function of T at P = 0.1 (black squares), 1 (red circles), 2.5 (heating scan, blue up triangles), 4 (green down triangles), and 5 (magenta left triangles) kbar. The LHS region of the dashed vertical line is the two-phase region with its phase separation between 3 and 4 kbar. The RHS region of the dotted vertical line is the one-phase region. All data in this figure were taken at SPINS.

the phase diagram shown in Figure 3, below ~ 190 K, the former three pressures are in the LDL phase, whereas the last two pressures are in the HDL phase. Figure 4 clearly shows that below 190 K, there is an evident density gap of ~ 0.04 g/cm³ between the density profiles at 0.1, 1, 2.5 kbar and the density profile at 4 kbar. This gap shows the phase separation between LDL and HDL. In this temperature range, the three density curves representing LDL phase are close to each other, which shows that the isothermal compressibility (χ_T) of the LDL phase is small. At 170 K, the density only changes by ~ 0.004 g/cm³ as pressure increases from 100 bar to 2.5 kbar. In contrast, in HDL phase, the density changes by ~ 0.02 g/cm³ as pressure increases from 4 to 5 kbar, which suggests a significantly larger χ_T . The huge difference of χ_T in LDL and HDL is due to the different local structures of LDL and HDL. The LDL has a tetrahedral hydrogen-bond structure extending to the second coordination shell. However, for the HDL, the second coordination shell collapses.³⁸ These features make the LDL

more rigid than the HDL. Such sharp distinction on χ_T fades out as entering the one-phase region, which suggests that the LDL and HDL phases mix in this region.

A previous study²¹ shows that at ambient pressure, for an 85% partially hydrated sample, the density minimum obscures and the maximum of the absolute value of the isobaric thermal expansion coefficient ($|\alpha_P|$) decreases as compared to the fully hydrated sample. Therefore, it is interesting to examine if a reduction of h can mitigate the phase transition at high pressures. Figure 5 shows the average density of the confined

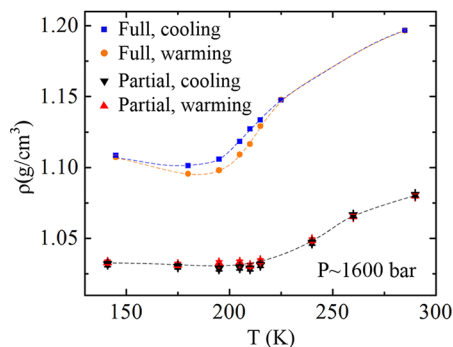


Figure 5. Density profiles of confined D_2O with warming (red up triangles) and cooling (black down triangles) scans for a partially hydrated sample at $P \sim 1600$ bar. It is seen that no hysteresis is found in this sample. We also plot the density profiles of confined D_2O with warming (orange circles) and cooling (blue squares) scans for the fully hydrated sample at $P \sim 1600$ bar for comparison. All data in this figure were taken at SPINS.

D_2O of an 80% partially hydrated sample at ~ 1.6 kbar with warming and cooling scans. Strikingly, the density hysteresis completely disappears in this sample. The disappearance of the density hysteresis in the partially hydrated sample is also observed at 1 and 2.5 kbar. Notice that both experimental and computer simulation studies show that the confined water has layer structure.^{8,39,40} According to Gallo et al.,⁸ the water confined in MCM-41 can be divided into two dynamically distinct parts in radial direction: bound water and free water. The bound water is a 3-Å-thick shell layer that coats to the hydrophilic surface of the silica cavity, whereas the free water is the water in the center part of the cavity. Because the water forms the shell layer first,⁴¹ the 20% lowering of h is mainly due to the reduction of the free water. Thus, in this partially hydrated sample, the amount of free water decreases by about 50% compared to its fully hydrated counterpart. The disappearance of the density hysteresis in the partially hydrated sample strongly suggests that (1) the free water, not the bound water, undergoes a liquid–liquid transition and (2) a well-developed hydrogen-bond network in free water is the necessary condition for water confined in MCM-41 to exhibit liquid–liquid transition.

Though the confined water system behaves differently from the bulk water due to the strong confinement, it is still interesting to compare our result to the theoretical and numerical predictions related to bulk water. Four scenarios have been proposed for the low-temperature phase behavior of liquid water,⁴² they are (1) the stability limit (SL) scenario;⁴³ (2) the liquid–liquid critical point (LLCP) scenario;⁵ (3) the singularity-free (SF) scenario;^{44–46} and (4) the critical-point free (CPF) scenario.⁴⁷ The phase diagram obtained here is qualitatively similar to the phase diagrams suggested by LLCP

scenario and SF scenario. In this study, we define the end point of the LLPT as the LLCP of the confined heavy water. The SF scenario suggests that no singularity at the end point of the LLPT.⁴⁴ To directly distinguish between these two scenarios, one may want to study the critical behavior of the LLPT end point. Nevertheless, the quasi-one-dimensional geometry in MCM-41 can strongly suppress any critical behavior.¹⁵ Thus, to measure the critical behaviors near the end point of LLPT is almost impossible. In fact, as the pressure approaching the critical pressure, the absolute value of the isobaric thermal expansion coefficient $|\alpha_p|$ of the confined D₂O exhibits no critical phenomenon.⁴⁸ Kumar et al. suggests another method to distinguish between these two scenarios: in the LLCP scenario, the maximum of C_p increases with the increase of pressure, whereas in the SF scenario, the maximum of C_p does not.²⁹ In ref 10, below the critical pressure, the maximum density difference increases from 0.010 g/cm³ at 1 bar to 0.017 g/cm³ at ~ 1 kbar. Considering the fact that the $|\alpha_p|$ increases only by 2.7% as P increases from 1 bar to ~ 1 kbar,⁴⁸ we conjecture that such big increases on maximum density difference as P increases from 1 bar to ~ 1 kbar is mainly due to the enhancement of the temperature lag, which indicates a larger C_p . Following this logic, we suggest that the LLCP scenario provides a better explanation. It is worth mention that, for bulk water, recent experimental and theoretical studies support the LLCP scenario rather than the SF scenario.^{49–51}

In summary, we investigate the average density of the deeply cooled heavy water confined in the MCM-41 over the pressure–temperature plane. By detecting the density hysteresis, we find that the transition in the system is a liquid–liquid transition, rather than a liquid–solid transition. The locus of the LLPT line is determined. Its end point, which locates at 1.29 ± 0.34 kbar and 213 ± 3 K, could be the LLCP according to the LLCP scenario. The locus of the Widom line is also estimated. Therefore, the phase diagram of the confined water system is obtained. In addition, we measure an 80% partially hydrated sample, and it shows that no transition appears in this sample even at high pressures. This result shows that it is the free water part, rather than the bound water part, of the confined water that undergoes a liquid–liquid transition.

■ ASSOCIATED CONTENT

● Supporting Information

The information about the MCM-41-S sample we used, the detailed derivations of the equations in this paper and the data analysis method. The Supporting Information is available free of charge on the ACS Publications website at DOI: 10.1021/acs.jpclett.5b00827.

■ AUTHOR INFORMATION

Corresponding Author

* E-mail: sowhsin@mit.edu.

Notes

The authors declare no competing financial interest.

■ ACKNOWLEDGMENTS

The research at MIT was supported by DOE grant DE-FG02-90ER45429. We acknowledge the support of the U.S. Department of Commerce in providing the beamtimes at NCNR. We thank Dr. K.-H. Liu and P. Le for their help in the experiment.

■ REFERENCES

- (1) Debenedetti, P. G. Supercooled and Glassy Water. *J. Phys.: Condens. Matter* **2003**, *15*, R1669–R1726.
- (2) Debenedetti, P. G.; Stanley, H. E. Supercooled and Glassy Water. *Phys. Today* **2003**, *56*, 40–46.
- (3) Angell, C. A. Supercooled Water. *Annu. Rev. Phys. Chem.* **1983**, *34*, 593–630.
- (4) Mishima, O.; Stanley, H. E. The Relationship between Liquid, Supercooled and Glassy Water. *Nature* **1998**, *396*, 329–335.
- (5) Poole, P. H.; Sciortino, F.; Essmann, U.; Stanley, H. E. Phase Behaviour of Metastable Water. *Nature* **1992**, *360*, 324–328.
- (6) Liu, K.-H.; Zhang, Y.; Lee, J.-J.; Chen, C.-C.; Yeh, Y.-Q.; Chen, S.-H.; Mou, C.-Y. Density and Anomalous Thermal Expansion of Deeply Cooled Water Confined in Mesoporous Silica Investigated by Synchrotron X-ray Diffraction. *J. Chem. Phys.* **2013**, *139*, 064502.
- (7) Bertrand, C. E.; Zhang, Y.; Chen, S.-H. Deeply-Cooled Water under Strong Confinement: Neutron Scattering Investigations and the Liquid–Liquid Critical Point Hypothesis. *Phys. Chem. Chem. Phys.* **2013**, *15*, 721–745.
- (8) Gallo, P.; Rovere, M.; Chen, S.-H. Dynamic Crossover in Supercooled Confined Water: Understanding Bulk Properties through Confinement. *J. Phys. Chem. Lett.* **2010**, *1*, 729–733.
- (9) Soper, A. K. Structural Transformations in Amorphous Ice and Supercooled Water and Their Relevance to the Phase Diagram of Water. *Mol. Phys.* **2008**, *106*, 2053–2076.
- (10) Zhang, Y.; Faraone, A.; Kamitakahara, W. A.; Liu, K.-H.; Mou, C.-Y.; Leão, J. B.; Chang, S.; Chen, S.-H. Density Hysteresis of Heavy Water Confined in a Nanoporous Silica Matrix. *Proc. Natl. Acad. Sci. U.S.A.* **2011**, *108*, 12206–12211.
- (11) Wang, Z.; Liu, K.-H.; Harriger, L.; Leão, J. B.; Chen, S.-H. Evidence of the Existence of the High-Density and Low-Density Phases in Deeply-Cooled Confined Heavy Water under High Pressures. *J. Chem. Phys.* **2014**, *141*, 014501.
- (12) Poole, P. H.; Sciortino, F.; Essmann, U.; Stanley, H. E. Spinodal of Liquid Water. *Phys. Rev. E* **1993**, *48*, 3799–3817.
- (13) Murata, K.-I.; Tanaka, H. General Nature of Liquid–Liquid Transition in Aqueous Organic Solutions. *Nat. Commun.* **2013**, *4*, 3844.
- (14) Murata, K.-I.; Tanaka, H. Liquid–Liquid Transition without Macroscopic Phase Separation in a Water–Glycerol Mixture. *Nat. Mater.* **2012**, *11*, 436–443.
- (15) Gelb, L.; Gubbins, K.; Radhakrishnan, R.; Sliwinski-Bartkowiak, M. Phase Separation in Confined Systems. *Rep. Prog. Phys.* **1999**, *62*, 1573–1659.
- (16) Mamontov, E.; Chu, X.-Q. Water–Protein Dynamic Coupling and New Opportunities for Probing It at Low to Physiological Temperatures in Aqueous Solutions. *Phys. Chem. Chem. Phys.* **2012**, *14*, 11573–11588.
- (17) Limmer, D. T.; Chandler, D. The Putative Liquid–Liquid Transition is a Liquid–Solid Transition in Atomistic Models of Water. *J. Chem. Phys.* **2011**, *135*, 134503.
- (18) Limmer, D. T.; Chandler, D. The Putative Liquid–Liquid Transition is a Liquid–Solid Transition in Atomistic Models of Water. II. *J. Chem. Phys.* **2013**, *138*, 214504.
- (19) Palmer, J. C.; Martelli, F.; Liu, Y.; Car, R.; Panagiotopoulos, A. Z.; Debenedetti, P. G. Metastable Liquid–Liquid Transition in a Molecular Model of Water. *Nature* **2014**, *510*, 385–388.
- (20) Liu, D.; Zhang, Y.; Chen, C.-C.; Mou, C.-Y.; Poole, P. H.; Chen, S.-H. Observation of the Density Minimum in Deeply Supercooled Confined Water. *Proc. Natl. Acad. Sci. U.S.A.* **2007**, *104*, 9570–9574.
- (21) Liu, D.; Zhang, Y.; Liu, Y.; Wu, J.; Chen, C.-C.; Mou, C.-Y.; Chen, S.-H. Density Measurement of 1-D Confined Water by Small Angle Neutron Scattering Method: Pore Size and Hydration Level Dependences. *J. Phys. Chem. B* **2008**, *112*, 4309–4312.
- (22) Kamitakahara, W. A.; Faraone, A.; Liu, K.-H.; Mou, C.-Y. Temperature Dependence of Structure and Density for D₂O Confined in MCM-41-S. *J. Phys.: Condens. Matter* **2012**, *24*, 064106.
- (23) See the Supporting Information for the description of the sample and the analysis model used in this study.

- (24) Liu, L.; Chen, S.-H.; Faraone, A.; Yen, C.-W.; Mou, C.-Y. Pressure Dependence of Fragile-to-Strong Transition and a Possible Second Critical Point in Supercooled Confined Water. *Phys. Rev. Lett.* **2005**, *95*, 117802.
- (25) Wang, Z.; Liu, K.-H.; Le, P.; Li, M.; Chiang, W.-S.; Leão, J. B.; Copley, J. R. D.; Tyagi, M.; Podlesnyak, A.; Kolesnikov, A. I.; Mou, C.-Y.; Chen, S.-H. Boson Peak in Deeply Cooled Confined Water: A Possible Way to Explore the Existence of the Liquid-to-Liquid Transition in Water. *Phys. Rev. Lett.* **2014**, *112*, 237802.
- (26) Oguni, M.; Kanke, Y.; Nagoe, A.; Namba, S. Calorimetric Study of Water's Glass Transition in Nanoscale Confinement, Suggesting a Value of 210 K for Bulk Water. *J. Phys. Chem. B* **2011**, *115*, 14023.
- (27) Nagoe, A.; Kanke, Y.; Oguni, M.; Namba, S. Findings of C_p Maximum at 233 K for the Water within Silica Nanopores and Very Weak Dependence of the T_{\max} on the Pore Size. *J. Phys. Chem. B* **2010**, *114*, 13940–13943.
- (28) Xu, L.; Kumar, P.; Buldyrev, S. V.; Chen, S.-H.; Poole, P. H.; Sciortino, F.; Stanley, H. E. Relation between the Widom Line and the Dynamic Crossover in Systems with a Liquid–Liquid Phase Transition. *Proc. Natl. Acad. Sci. U.S.A.* **2005**, *102*, 16558–16562.
- (29) Kumar, P.; Franzese, G.; Stanley, H. E. Predictions of Dynamic Behavior under Pressure for Two Scenarios to Explain Water Anomalies. *Phys. Rev. Lett.* **2008**, *100*, 105701.
- (30) Franzese, G.; Stanley, H. E. The Widom Line of Supercooled Water. *J. Phys.: Condens. Matter* **2007**, *19*, 205126.
- (31) Bianco, V.; Franzese, G. Critical Behavior of a Water Monolayer under Hydrophobic Confinement. *Sci. Rep.* **2014**, *4*, 4440.
- (32) Kesselring, T. A.; Franzese, G.; Buldyrev, S. V.; Herrmann, H. J.; Stanley, H. E. Nanoscale Dynamics of Phase Flipping in Water near its Hypothesized Liquid–Liquid Critical Point. *Sci. Rep.* **2012**, *2*, 474.
- (33) Giovambattista, N.; Loerting, T.; Lukanov, B. R.; Starr, F. W. Interplay of the Glass Transition and the Liquid–Liquid Phase Transition in Water. *Sci. Rep.* **2012**, *2*, 390.
- (34) Johari, G. P.; Hallbrucker, A.; Mayer, E. Two Calorimetrically Distinct States of Liquid Water Below 150 K. *Science* **1996**, *273*, 90–92.
- (35) Johari, G. P.; Hallbrucker, A.; Mayer, E. The Glass–Liquid Transition of Hyperquenched Water. *Nature* **1987**, *330*, 552–553.
- (36) Smith, R. S.; Kay, B. D. The Existence of Supercooled Liquid Water at 150 K. *Nature* **1999**, *398*, 788–791.
- (37) Velikov, V.; Borick, S.; Angell, C. A. The Glass Transition of Water, Based On Hyperquenching Experiments. *Science* **2001**, *294*, 2335–2338.
- (38) Soper, A. K.; Ricci, M. A. Structures of High-Density and Low-Density Water. *Phys. Rev. Lett.* **2000**, *84*, 2881–2884.
- (39) Schreiber, A.; Ketelsen, I.; Findenegg, G. H. Melting and Freezing of Water in Ordered Mesoporous Silica Materials. *Phys. Chem. Chem. Phys.* **2001**, *3*, 1185–1195.
- (40) Svergun, D. I.; Richard, S.; Roch, M. H.; Sayers, Z.; Kuprin, S.; Zaccai, G. Protein Hydration in Solution: Experimental Observation by X-ray and Neutron Scattering. *Proc. Natl. Acad. Sci. U.S.A.* **1998**, *95*, 2267–2272.
- (41) Grunberg, B.; Emmler, T.; Gedat, E.; Shenderovich, I.; Findenegg, G. H.; Limbach, H.-H.; Buntkowsky, G. Hydrogen Bonding of Water Confined in Mesoporous Silica MCM-41 and SBA-15 Studied by ^1H Solid-State NMR. *Chem.–Eur. J.* **2004**, *10*, 5689–5696.
- (42) Stokely, K.; Mazza, M. G.; Stanley, H. E.; Franzese, G. Effect of Hydrogen Bond Cooperativity on the Behavior of Water. *Proc. Natl. Acad. Sci. U.S.A.* **2010**, *107*, 1301–1306.
- (43) Speedy, R. J. Limiting Forms of the Thermodynamic Divergences at the Conjectured Stability Limits in Superheated and Supercooled Water. *J. Phys. Chem.* **1982**, *86*, 3002–3005.
- (44) Sastry, S.; Debenedetti, P. G.; Sciortino, F.; Stanley, H. E. Singularity-Free Interpretation of the Thermodynamics of Supercooled Water. *Phys. Rev. E* **1996**, *53*, 6144–6154.
- (45) Stanley, H. E. A Polychromatic Correlated-Site Percolation Problem with Possible Relevance to the Unusual Behaviour of Supercooled H_2O and D_2O . *J. Phys. A: Math. Gen.* **1979**, *12*, L329–L337.
- (46) Stanley, H. E.; Teixeira, J. Interpretation of the Unusual Behavior of H_2O and D_2O at Low Temperatures: Tests of a Percolation Model. *J. Chem. Phys.* **1980**, *73*, 3404–3422.
- (47) Angell, C. A. Insights into Phases of Liquid Water from Study of Its Unusual Glass-Forming Properties. *Science* **2008**, *319*, 582–587.
- (48) Liu, D. Studies of Liquid–Liquid Phase Transition and Critical Phenomena in Supercooled Confined Water by Neutron Scattering. Ph.D. Thesis, Massachusetts Institute of Technology, 2008.
- (49) Holten, V.; Bertrand, C. E.; Anisimov, M. A.; Sengers, J. V. Thermodynamics of Supercooled Water. *J. Chem. Phys.* **2012**, *136*, 094507.
- (50) Holten, V.; Anisimov, M. A. Entropy-Driven Liquid–Liquid Separation in Supercooled Water. *Sci. Rep.* **2012**, *2*, 713.
- (51) Mishima, O. Volume of Supercooled Water under Pressure and the Liquid–Liquid Critical Point. *J. Chem. Phys.* **2010**, *133*, 144503.